Direct Visualization of A-, P-, and E-Site Transfer RNAs in the *Escherichia coli* Ribosome

Rajendra K. Agrawal, Pawel Penczek, Robert A. Grassucci, Yanhong Li, ArDean Leith, Knud H. Nierhaus, Joachim Frank*

Transfer RNA (tRNA) molecules play a crucial role in protein biosynthesis in all organisms. Their interactions with ribosomes mediate the translation of genetic messages into polypeptides. Three tRNAs bound to the *Escherichia coli* 70S ribosome were visualized directly with cryoelectron microscopy and three-dimensional reconstruction. The detailed arrangement of A- and P-site tRNAs inferred from this study allows localization of the sites for anticodon interaction and peptide bond formation on the ribosome.

In protein biosynthesis, the tRNAs, carrying covalently attached amino acids which are the building blocks of the polypeptide chain, are known to occupy successively three sites on the ribosome: one for the incoming aminoacyl tRNA (A site), one for the peptidyl tRNA (P site) (*1*), and the third for the exiting tRNA (E site) (*2*, *3*). These binding sites account for the codon-anticodon interaction between mRNA and tRNA, the correct positioning of tRNA acceptor and donor arms during peptide bond formation, and the movement of mRNA relative to the ribosome. Studies conducted during the past two decades clearly place the anticodon and aminoacyl ends of A- and P-site tRNAs onto the 30S and 50S subunits of the *E. coli* ribosome, respectively. Although some attempts have been made to map the tRNA binding site on the 30S ribosomal subunit (*4*), no studies have succeeded in directly visualizing tRNA molecules bound to the 70S ribosome (comprising the 30S and 50S subunits). We have obtained a three-dimensional (3D) cryoelectron microscopy map of a poly(U) programmed *E. coli* 70S ribosome in which the sites are occupied by three deacylated $tRNA^{Phe}$ molecules, and we have computed a difference map by comparison with the previous cryoreconstruction of an unoccupied (naked) ribosome (*5*). All three tRNAs are clearly distinguishable and occur in an open configuration, with the A- and P-site tRNAs enclosing an angle of about 160°. In addition, a conformational change of the tRNA relative to that seen in its crystal structure (*6*) was observed. The physiological relevance of our findings is supported by the observation (*7*, *8*) that the positions of the deacylated tRNAs in 70S ribosomes are close to those with aminoacyl or peptidyl tRNAs.

The difference map obtained by subtraction of the map of the naked 70S ribosome (*5*) from the new reconstruction of the $tRNA^{Phe}$-bound 70S ribosome (*9*) shows a mass of density with complex shape in the intersubunit space (Fig. 1 and Fig. 2, A and B), which can be readily interpreted (Fig. 1 and Fig. 2, C and D) as an arrangement of three tRNA molecules that appear to be partially fused because of resolution limitations. The locations of three elbow-shaped bulges observed in the difference mass, interpreted as elbow regions of the three tRNAs, were used as the main guide for fitting of the atomic models of tRNA. In accordance with the existing body of knowledge, we identify the tRNA molecule closest to the L7/L12 stalk [for identification of this and other morphological markers, see

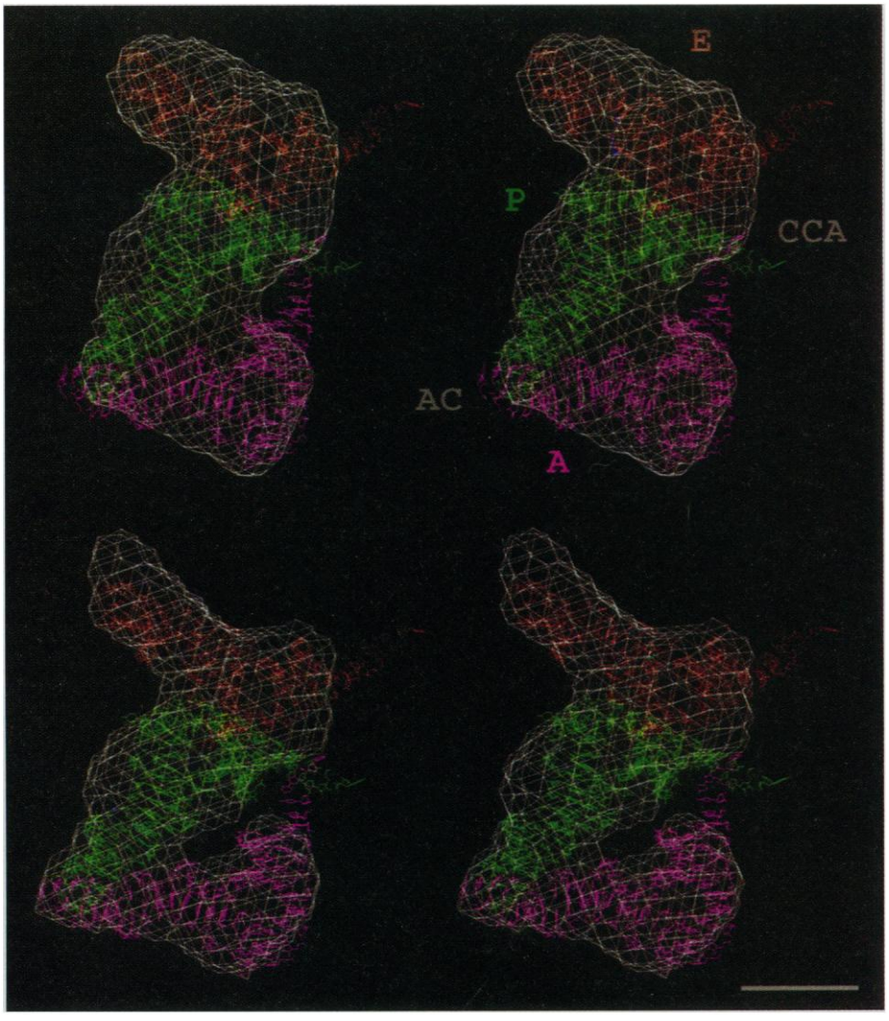

Fig. 1. Stereoview representation of the difference map (white contour) found in the intersubunit space of the ribosome (also see Fig. 2, A and B) and its interpretation in terms of the crystal structure of tRNA (*6*). A, A site (pink); P, P site (green); E, E site (brown) tRNA. AC, anticodon portion; CCA, aminoacyl ends of the A- and P-site tRNAs. (**Upper portion**) CTF-corrected difference map. (**Lower portion**) Difference map without CTF correction, showing that the fit extends to the anticodon ends when high-resolution features are enhanced. Scale bar, 25 Å.

R. K. Agrawal, P. Penczek, R. A. Grassucci, Y. Li, A. Leith, Wadsworth Center, New York State Department of Health, Empire State Plaza, Albany, NY 12201–0509, USA.
K. H. Nierhaus, Max-Planck-Institut für Molekulare Genetik, Ihnestrasse 73, D-14195 Berlin, Germany.
J. Frank, Wadsworth Center, New York State Department of Health, Empire State Plaza, Albany, NY 12201–0509, USA, and Department of Biomedical Sciences, State University of New York at Albany, 1400 Washington Avenue, Albany, New York 12222, USA.
*To whom correspondence should be addressed.

(5)] as the A site, the one next to it as the P site, and the one in the close vicinity of the L1 protein, farthest away from the A-site tRNA, as the E site. This interpretation immediately places the anticodon loops and CCA ends of A- and P-site tRNAs in close proximity to each other, respectively. With this positioning of A- and P-site tRNAs, the remaining mass tightly accommodates another tRNA molecule, interpreted as the E site. We believe that the reason the CCA ends are not visible in the difference mass is because they are single-stranded, with a thickness below the resolution limit (25 Å). Some of the remaining discrepancies observed in this fitting may be due to the mass of density contributed by the subsets of the ribosomal populations present in their hybrid (A/P and P/E) states (*10*). The absence of any detectable negative difference peaks in the immediate vicinity of the difference mass makes it unlikely that part of the mass is due to a conformational change of the ribosome. Additionally, the fitting of the atomic model of tRNA to our experimental data revealed a conformational change in its ribosome-bound state as compared with the crystal structure (*6*): The anticodon arm of the A-site tRNA was found to be bent in the middle (Fig. 2), out of the plane of the molecule, toward the side of the D loop. Similar bends in the anticodon arm of tRNAs have been observed in the structures of tRNA-tRNA synthetase complexes (*11*). However, accounting for this change would move the inferred position of the CCA end only slightly. The difference map also shows a separate, smaller mass that is possibly due to a conformational change in the region of the L7/L12 stalk of the 50S subunit.

The mutual arrangement of the A- and P-site tRNAs differs from both "R" and "S" configurations (*12*) in that their planes enclose an angle of about 160° [compare with (*5*, *13*, *14*)], whereas the position of the E-site tRNA appears to exclude codon-anticodon contact [compare with (*15*)]. However, the positions we have found satisfy most of the data from cross-linking (*13*, *16*, *17*) and electron microscopic mapping (*4*, *18*). The anticodon ends of the A- and P-site tRNAs meet at the interface side of the small subunit's "neck" region, in close vicinity to the channel previously seen (*5*) but on the L7/L12 side of the channel rather than toward the platform [compare with (*5*)]. The elbow of the A-site tRNA is perched in the cavity formed by the intersubunit bridge, the base of the L7/L12 stalk, and the interface canyon. The position of the P-site tRNA is such that the anticodon stem-loop side of the elbow touches the 30S subunit head and the rim of the platform, and the CCA end points toward the entry of the tunnel situated at the bottom of the interface canyon, approximately as postulated by Frank and co-workers (*5*). This position agrees with chemical protection

Table 1. Comparison of our results with FRET (*20*) measurements. Dash indicates no data available.

A-site tRNA residue number	P-site tRNA residue number	Distance measurements (Å)	
		FRET	This study
37 (anticodon loop)	37	24 ± 4	15
37	16, 17 (D loop)	46 ± 12	43
16, 17	37	38 ± 10	36
16	16, 17	35 ± 9	44,48
17	16, 17	35 ± 9	51,55
8	8	26 ± 4	28
76 (CCA end)	76	—	12

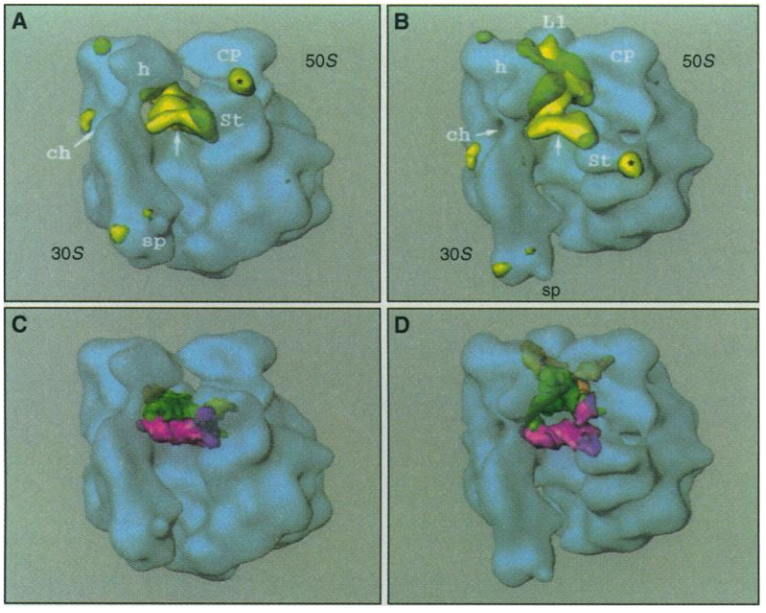

Fig. 2. CTF-corrected difference map (yellow, appearing green in regions of perspective overlap) superimposed on the ribosome (shown in blue as transparent map). Morphological features of the 50S subunit: CP, central protuberance; L1, L1 protein; St, L7/L12 stalk. Morphological features of the 30S subunit; h, head; ch, channel; sp, spur. (**A**), side view; (**B**), top view [generated from (A) by rotation of the map by 35° around the horizontal axis]. The arrow below the difference map points to a bend in the region interpreted as the anticodon arm of the A-site tRNA and the asterisk indicates the conformational change in the L7/L12 stalk region. (**C** and **D**) Interpretation of the difference map viewed as in (A and B) in terms of three tRNA molecules, each represented by the envelope of a 5 Å resolution map.

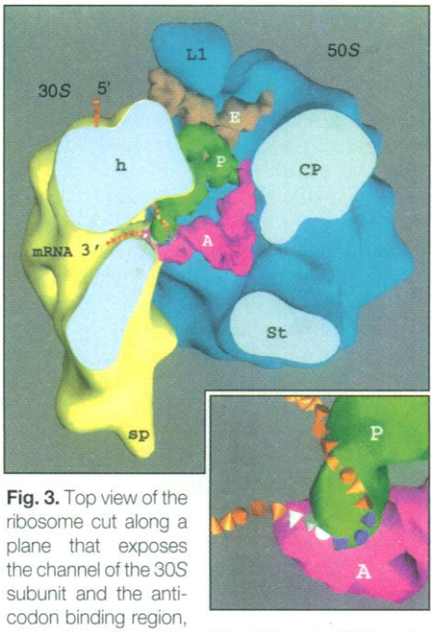

Fig. 3. Top view of the ribosome cut along a plane that exposes the channel of the 30S subunit and the anticodon binding region, and schematic outline of the inferred mRNA pathway. Morphological features are marked as in Figs. 1 and 2. Ribonucleotide bases are represented by cones whose orientations follow the pitch of 11 bases per 360°, except in the region of anticodon binding (white and purple) where an additional 70° turn is accommodated by a stretch of four bases (that is from the center of the A-site codon to the center of the P-site codon), as necessitated by the orientations of the A and P tRNAs. Inset shows a magnified view of the codon-anticodon interaction region.

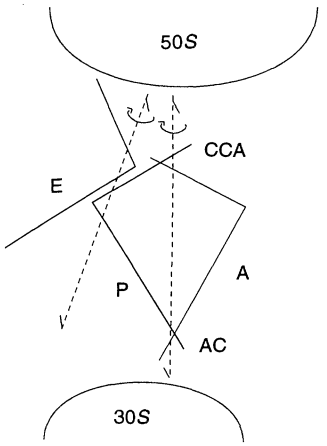

Fig. 4. Schematic diagram depicting the inferred movements of the tRNA from A to P site and from P to E site. A→P is a combination of a 160° rotation and an upward shift along the rotation axis by 9 Å. P→E is a combination of a 145° rotation and an upward shift by approximately 20 Å. The positions of the corresponding two left-handed screw axes are indicated by dashed lines. CCA, CCA ends; AC, anticodons of A- and P-site tRNAs. For both A- and E-site tRNAs, the D loop in the elbow region faces the viewer, whereas it faces away for the P-site tRNA.

and cross-linking data (*7, 8, 16*). We find the E-site tRNA in a topographically distinct position, with the D-loop side facing (and almost touching) the D-loop side of the aminoacyl arm of the P-site tRNA, such that the inner bend of the molecule faces the L1 protein. Its CCA end appears to occupy the space between the L1 protein and the central protuberance of the 50S subunit, while its anticodon arm spans the space between the L1 protein and the platform of the 30S subunit (Fig. 3), which is in good agreement with chemical protection (*7*) and protein cross-linking (*19*) data.

The arrangement obtained by fitting three copies of the atomic model of the tRNA (Fig. 1 and Fig. 2, C and D) into the difference map (Fig. 1 and Fig. 2, A and B) agrees with much of the fluorescence-resonance-energy-transfer (FRET) data (*20*) (Table 1). Discrepancies occur in the distances between the D loops and residues 37 of A- and P-site tRNAs, which are the regions that would be most affected by the conformational change in the A-site tRNA.

The relative position between A- and P-site tRNAs can be described as a rotation by 160° around the anticodon-CCA axis and a simultaneous shift by approximately 9 Å. A similar staggered arrangement between A- and P- site tRNAs has been postulated by Lim and co-workers (*12*), albeit with a smaller angle between the molecules. Thus, when both sites are occupied, the 3′ end of the A-site tRNA anticodon is in close proximity (slightly below) to the 5′ end of the P-site tRNA anticodon. When the natural conformation of mRNA and the crystal structure of tRNA are considered, this arrangement would imply that to allow cogent hydrogen bonding to be formed for the two adjacent codons, the mRNA may undergo a twist of close to 70°. The resulting strain must be absorbed by the six consecutive base pairings, which include the wobble bases of the anticodons (Fig. 3). If the tRNA molecule is constrained to move along the A→P path outlined in Fig. 4, by an as yet unknown mechanism, then the advance of the mRNA by one codon (*21*) could be effected by a force that acts on the A-site tRNA. The L7/L12 stalk, whose base is now found in close proximity to the A-site tRNA elbow, has been long suspected to have an active role in translocation (*22*). Indeed, our data indicate a conformational change in that region of the map (Fig. 2, A and B) where the stalk seems to be extended away from the body of the ribosome. Experiments with a translationally defined system using aminoacyl and peptidyl tRNAs may further refine the data presented in this study.

REFERENCES AND NOTES

1. J. D. Watson, *Bull. Soc. Chim. Biol.* **46**, 1399 (1964).
2. H.-J. Rheinberger, H. Sternbach, K. H. Nierhaus, *Proc. Natl. Acad. Sci. U.S.A.* **76**, 5310 (1981).
3. R. A. Grajevskaja, Yu. V. Ivanov, E. M. Saminsky, *Eur. J. Biochem.* **128**, 47 (1982); S. V. Kirrilov, E. M. Makarov, Yu. P. Semenkov, *FEBS Lett.* **157**, 91 (1983); R. Lill, J. M. Robertson, W. Wintermeyer, *Biochemistry* **25**, 3245 (1984).
4. P. Gornicki, K. Nurse, W. Hellmann, M. Boublik, J. Ofengand, *J. Biol. Chem.* **259**, 10493 (1984); T. Wagenknecht, J. Frank, M. Boublik, K. Nurse, J. Ofengand, *J. Mol. Biol.* **203**, 753 (1988).
5. J. Frank *et al.*, *Nature* **376**, 441 (1995).
6. S.-H. Kim *et al.*, *Science* **185**, 435 (1974); J. L. Sussman and S.-H. Kim, *Biochem. Biophys. Res. Commun.* **68**, 89 (1976); J. L. Sussman, S. R. Holbrook, R. W. Warrant, G. M. Church, S.-H. Kim, *J. Mol. Biol.* **123**, 607 (1978).
7. D. Moazed and H. F. Noller, *Cell* **57**, 585 (1989).
8. ———, *J. Mol. Biol.* **211**, 135 (1990).
9. The *E. coli* $tRNA^{Phe}$ was radiolabeled at the 5′ end, as described by Silberklang and co-workers (*23*), and its binding saturation curve was studied (*2*). A 32-fold molar excess of $tRNA^{Phe}$ was required to saturate the poly(U) coded ribosome when all three sites were supposed to be occupied (*2, 3*). Activated 30*S* tight-couple subunits (50 pmol) were incubated with poly(U) (10 μg) in 10 μl of buffer containing 50 mM tris-HCl (pH 7.8), 15 mM magnesium acetate, 160 mM NH_4Cl, and 5 mM β-mercaptoethanol. Then an equimolar amount of the 50*S* tight-couple subunit was added (total volume 15 μl) and further incubated under the same conditions for 60 min. *Escherichia coli* $tRNA^{Phe}$ (1.6 nmol) was added in the reaction mixture (total volume 25 μl) and the incubation was continued for another 30 min. The reaction mixture was subjected to centrifugation (10 to 30% sucrose gradient) in the same buffer to purify ribosomes from the unbound tRNAs, mRNAs, and ribosomal subunits. Cryogrids were prepared at a 0.85 A_{260}/ml concentration of the sample. Two sets of ribosome projections were obtained by cryoelectron microscopy (Philips EM 420): A total of 855 projections were obtained with 2.0-μm defocus and a total of 1636 projections were obtained with 2.5-μm defocus. The angles were determined with the use of a projection matching procedure (*24*) with the control (*5*). Two volumes were calculated, one for each set of projections at 2.0-μm and 2.5-μm defocus, respectively, and combined by means of a contrast transfer function (CTF) correction procedure (J. Zhu, P. Penczek, R. Schröder, J. Frank, in preparation). The difference map was formed by subtraction of the control reconstruction of the naked ribosome (*5*) from the new merged reconstruction of the ribosome-tRNA complex.
10. D. Moazed and H. F. Noller, *Nature* **342**, 142 (1989); H. F. Noller *et al.*, in *The Ribosome, Structure, Function and Evolution*, W. E. Hill *et al.*, Eds. (American Society for Microbiology, Washington, DC, 1990), pp. 73–92.
11. M. A. Rould, J. J. Perona, D. Söll, T. A. Steitz, *Science* **246**, 1135 (1989); M. Ruff *et al.*, *ibid.* **252**, 1682 (1991).
12. V. Lim *et al.*, *Nucleic Acids Res.* **20**, 2627 (1992).
13. R. Brimacombe, *Eur. J. Biochem.* **230**, 365 (1995).
14. H. Stark *et al.*, *Structure* **3**, 815 (1995).
15. K. H. Nierhaus, *Biochemistry* **29**, 4997 (1990).
16. R. A. Zimmermann, C. L. Thomas, J. Wower, in *The Ribosome, Structure, Function and Evolution*, W. E. Hill *et al.*, Eds. (American Society for Microbiology, Washington, DC, 1990), pp. 331–347.
17. J. Wower, K. V. Rosen, S. S. Hixon, R. A. Zimmermann, *Biochimie* **76**, 1235 (1994).
18. G. Stöffler and M. Stöffler-Meilicke, in *Structure, Function and Genetics of Ribosomes*, B. Hardesty and G. Krammer, Eds. (Springer-Verlag, New York, 1986), pp. 28–46; M. Oakes, E. Henderson, A. Scheinman, M. Clark, J. A. Lake, *ibid.*, pp. 47–67.
19. J. Wower, P. Scheffer, L. A. Sylvers, W. Wintermeyer, R. A. Zimmermann, *EMBO J.* **12**, 617 (1993).
20. A. E. Johnson, H. J. Adkins, E. A. Matthews, C. R. Cantor, *J. Mol. Biol.* **156**, 113 (1982); H. Paulsen, J. M. Robertson, W. Wintermeyer, *ibid.* **167**, 411 (1983).
21. D. Beyer, E. Skripkin, J. Wadzak, K. H. Nierhaus, *J. Biol. Chem.* **269**, 30713 (1994).
22. D. P. Burma, S. Srivastava, A. K. Srivastava, S. Mahanti, D. Dash, in *Structure, Function and Genetics of Ribosomes*, B. Hardesty and G. Krammer, Eds. (Springer-Verlag, New York, 1986), pp. 438–453; A. Liljas and A. T. Gudkov, *Biochimie* **69**, 1043 (1987); W. Moller, *ibid.* **73**, 1093 (1991); A. V. Oleinkov, B. Perroud, B. Wang, R. R. Traut, *J. Biol. Chem.* **268**, 917 (1993).
23. M. Silberklang, A. M. Gillum, U. L. RajBhandary, *Methods Enzymol.* **59**, 58 (1979).
24. P. Penczek, R. Grassucci, J. Frank, *Ultramicroscopy* **53**, 251 (1994).

25. Supported by NIH grants 1R01 GM29169 and P41 RR01219 and by NSF grant BIR 9219043. We thank S. Srivastava for helpful suggestions and discussions and T. Wagenknecht for a critical reading of the manuscript and suggestions. Coordinates of the complex formed by three copies of $tRNA^{Phe}$ as determined by fitting have been deposited in the Brookhaven Protein Data Bank, with tracking number T7700. The 3D density maps of occupied and unoccupied ribosomes and their difference map will be made available on the World Wide Web site www.wadsworth.org.

2 November 1995; accepted 21 December 1995